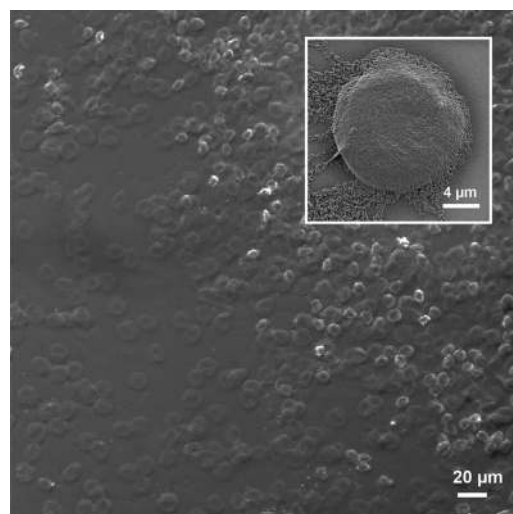


Microfluidic Production of Alginate Hydrogel Particles for Antibody Encapsulation and Release^a

Linus Mazutis,* Remigijus Vasiliauskas, David A. Weitz

Owing to their biocompatibility and reduced side effects, natural polymers represent an attractive choice for producing drug delivery systems. Despite few successful examples, however, the production of biopolymer-based particles is often hindered by considerable technical challenges mainly associated with high viscosity of polymer fluids. In this work, we present a microfluidic approach for production of alginate-based particles carrying encapsulated antibodies. We use a triple-flow microdevice to induce hydrogel formation inside droplets before their collection off-chip. The fast mixing and gelation process produced alginate particles with a unique biconcave shape and dimensions approaching those of mammalian cells. We show slow and fast dissolution of particles in different buffers and record controlled antibody release over time.



1. Introduction

Drug delivery systems based on natural biodegradable polymers are attractive agents for improved delivery, stabilization and prolonged release of encapsulated drugs.^[1] In many cases the techniques used for their production rely on mechanical stirring^[2] or spray-coagulation methods.^[3]

L. Mazutis, R. Vasiliauskas

Vilnius University Institute of Biotechnology, Vilnius LT-02241, Lithuania

E-mail: linas.mazutis@bti.vu.lt

L. Mazutis, D. A. Weitz

Harvard University, School of Engineering and Applied Sciences, Cambridge MA 02138, USA

These methods, although efficient, produce polydisperse drug particles and give a poor control over their size and shape. In this respect, droplet microfluidics provides a valuable tool for encapsulation of various biologicals and chemicals into highly monodisperse pico- and nanoliter volume droplets.^[4] Numerous examples reported to date have exploited droplet microfluidics to produce single^[5] and double emulsions,^[6] as well as various types of particles composed of responsive polymers^[7] and biodegradable materials.^[8] In this context, alginate, a natural polysaccharide derived from brown algae, is an attractive biomaterial for different applications in medical sciences.^[9] Due to their excellent biocompatibility alginate-based hydrogels are highly promising candidates for use as drug delivery systems^[10] or as biomedical implants.^[11] Indeed, much effort has been dedicated to producing different types of alginate hydrogel droplets and particles. For example, Huang et al., showed alginate droplet production using

^aSupporting Information is available online from the Wiley Online Library or from the author.

T-junction geometry, but the resultant bimodal distribution required an additional step of separation.^[12] Others, have generated alginate droplets on-chip, while inducing an “external gelation” process in bulk.^[13,14] Others, have employed capillary devices to produce alginate-based double emulsions,^[15] Janus particles^[16] and hydrogel beads carrying encapsulated cells.^[17,18] However, in all systems reported to date alginate hydrogel particles are relatively large in size ($\approx 50\text{--}200\ \mu\text{m}$), thereby reducing the scope of potential applications.^[19,20] For example, the use of microparticles as drug carriers requires their dimensions to be reduced to those of a cell ($\approx 10\ \mu\text{m}$). In particular, the reduced size should facilitate prolonged circulation in the blood and provide better encapsulation conditions of single cells. Indeed, production of smaller particles approaching the dimensions of a cell has been challenging due to the relatively high viscosity of alginate solutions ($>10\ \text{cP}$) and poor control over the polymerization kinetics. The latter difficulty is associated with fast gelation process triggered by divalent ions,^[21] therefore complicating both, production of monodisperse droplets as well as delivery of biological compounds into the droplets.^[19,22] A further requirement for drug-loaded particles is their biocompatibility, showing no adverse interactions with biomolecules, cells and tissues.

Here, we present a microfluidic approach for production of alginate hydrogel particles of biconcave (pancake) shape having the size resembling to those of mammalian cells ($\approx 10\ \mu\text{m}$). Using a microfluidic device with a characteristic flow-focusing junction that facilitates the break-up of viscous fluids into monodisperse droplets, we established the conditions for robust production of homogeneous alginate particles over extended periods of time. The size and shape of particles was governed by the cross-section of droplet stabilization channel: due to fast mixing and gelation of the liquid streams the resulting microgel particles acquired unique biconcave shape resembling the red blood cells. Loading alginate particles with fluorescently labeled antibodies allowed us to evaluate their release over time in different aqueous buffers. Finally, we tested the biocompatibility of alginate particles in the whole blood sample derived from laboratory rodents.

2. Results and Discussion

2.1. Microfluidics Chip Design

Initially, we tested alginate droplet production following principles reported previously,^[19,22] however, we could not recover alginate particles due to premature polymerization on-chip. We also tested alginate particle production by passively fusing alginate droplets with droplets containing Ca^{2+} ions,^[16,23] but this approach led to poor control over the monodispersity of the emulsion. Due to these

difficulties, we aimed to create a simple and robust system that would allow production of alginate particles over long periods of time for encapsulation of biologically active molecules such as antibodies or other therapeutic proteins. Using soft lithography, we created a microfluidic chip containing three aliquot inlets that merge into a single channel upstream of the flow-focusing junction (FFJ) as shown in Figure 1.

The channel downstream from the FFJ was $1\ 000\ \mu\text{m}$ long to allow interface stabilization by surfactant before the droplets collide and flow into the collection tube. During the course of droplet production, we noticed that viscosity differences of three fluids trigger complex flow instabilities resulting in polydisperse droplets. To prevent this from happening we incorporated fluid resistors for each aqueous phase ($R_h = 19.2\ \text{mPa}\ \text{s} \cdot \text{m}^{-3}$), so that their hydrodynamic resistances are considerably higher than that of the collection channel ($R_h = 3.2\ \text{mPa}\ \text{s} \cdot \text{m}^{-3}$).

In addition, we utilized a nozzle having a constriction of $10\ \mu\text{m}$ wide, which facilitated the pinch-off of viscous fluids into monodisperse droplets. To validate the functionality of the microfluidics device, we tested alginate droplet production using different flow rates and alginate concentrations (Supplementary Figure S1). Stable droplet production was achieved up to 2% (w/w) alginate, above which the viscosity of the alginate solution became too high making the droplet production process unstable (Figure 1c). To prevent premature hydrogel formation inside the microfluidic chip, a stream of water was introduced between the CaCl_2 and alginate solutions. However, fast diffusion of small Ca^{2+} ions through the thin layer of middle stream could induce premature alginate polymerization and eventually prevent droplet production. The distance of transverse diffusion, x , between two laminar streams can be described as $\langle x^2 \rangle = 2Dt$, where D is diffusion constant of a solute and t is a time that it takes for the solute from one liquid stream to diffuse into a second stream. We found that when using a microchannel of $80\text{--}100\ \mu\text{m}$ long and $10\ \mu\text{m}$ deep, the middle phase had to be $\geq 5\ \mu\text{m}$ thick to prevent premature alginate polymerization on-chip (Figure 1).

2.2. Alginate Droplet Production

Having established the design of a microfluidic chip, we tested production of alginate droplets using different flow regimes. Stable alginate droplet production was achieved when the flow rate for the continuous phase was at least two times higher than the total flow rate of the dispersed phases. Using a total flow rate for the dispersed phase of $100\text{--}150\ \mu\text{L} \cdot \text{h}^{-1}$, and for the continuous phase of $200\text{--}300\ \mu\text{L} \cdot \text{h}^{-1}$, allowed reproducible alginate droplet production over a period of a few hours. However, independently of the flow regimes used, priming of the

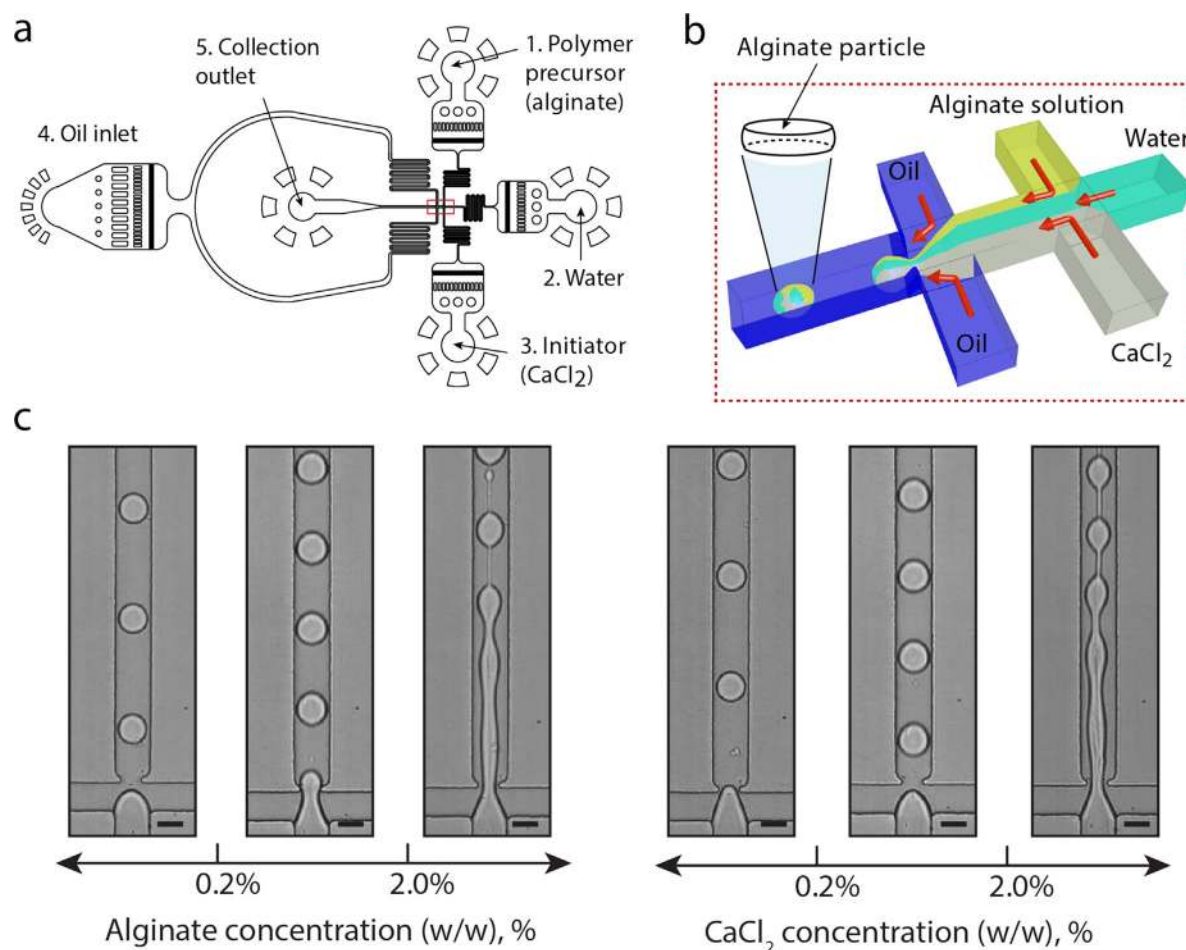


Figure 1. Design and operation of microfluidics chip. (a) The device consists of three inlets for, (1) polymer precursor (alginate), (2) water phase, (3) initiator (CaCl_2), (4) continuous phase, and (5) collection outlet. The channels for dispersed and continuous phases merge into a single channel (red square), where droplet generation takes place. (b) Graphical schematics depicting droplet generation using three aliquots (alginate solution, water, and CaCl_2) and oil (blue). (c) Droplet generation at different alginate and CaCl_2 concentrations. Droplet generation is stable for hours of continuous operation when alginate and CaCl_2 concentrations are below 2%; above this value droplet production becomes unstable due to fast polymerization and increased viscosity of alginate solution. Scale bars, 20 μm .

fluids was critically important. To prevent premature alginate polymerization on-chip, and thus clogging of the channels, the middle stream (water) had to be first injected into the chip and after the flow was stabilized ($\approx 3\text{--}5$ min), infusion of alginate and CaCl_2 solutions could follow.

We tested droplet production using different CaCl_2 concentrations ranging from 0.1 to 5% (w/w) dissolved in water (Figure 1c). At the lowest concentrations tested (0.1%) alginate droplets remained in a liquid form and did not polymerize into hydrogel. By contrast, at CaCl_2 concentrations between 2 and 5%, gelation occurred during the droplet pinch-off process inducing the formation of a pearl-like train (string), similar to the report previously.^[24] In the middle regime (0.5–1.0% CaCl_2) polymerization occurred within few milliseconds inside the droplets (immediately after the pinch-off process) before their collection off-chip.

Under these conditions, generation of monodisperse droplets was stable over extended periods of time. Increasing the total viscosity of the aqueous phase, however, induced jetting and undesirable polydispersity of the droplets.

Using our system polydispersity (coefficient of variation $\approx 20\%$) became pronounced when the alginate concentration was higher than 2% (w/w) or when the total viscosity of the aqueous phase reached ≈ 20 cP. The jetting could be partly suppressed by using a mineral oil of higher dynamic viscosity (≈ 15 cP), yet reliable production of particles was impossible due to pressure build-up and collapse of the microfluidic device. The use of FC-40 carrier oil (3.4 cP), however, was optimal allowing production of monodisperse droplets over a period of a few hours. Interestingly, when using 1% alginate solution the obtained hydrogel particles had biconcave (pancake) shape

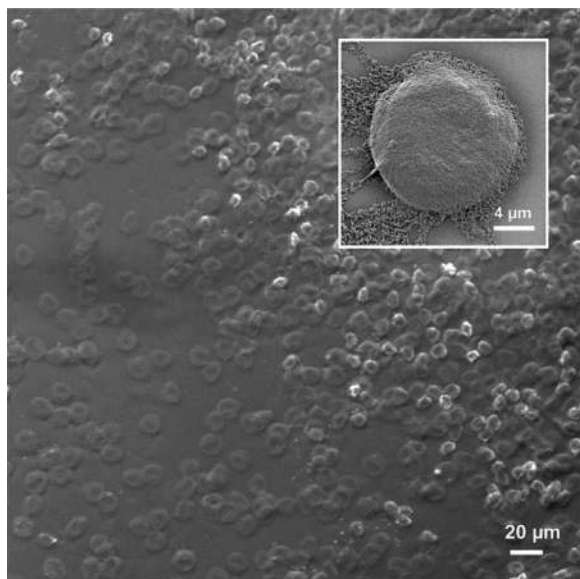


Figure 2. The shape of alginate hydrogel particles. Alginate particles produced with $10\ \mu\text{m}$ deep microfluidics chip using the flow rates: $30\ \mu\text{L}\cdot\text{h}^{-1}$ for alginate 1% (w/w) solution, $40\ \mu\text{L}\cdot\text{h}^{-1}$ for H_2O , $30\ \mu\text{L}\cdot\text{h}^{-1}$ for CaCl_2 and $300\ \mu\text{L}\cdot\text{h}^{-1}$ for FC40 oil. Alginate particles were placed on a microscope cover slip and imaged under the bright field microscope. The characteristic biconcave shape of resulting particles is clearly visible. Inset: scanning electron microscopy image of a single alginate particle after 48 h of incubation in physiological buffer. Note the disintegration of the alginate particle.

resembling red blood cells (Figure 2). The characteristic shape of resulting particles was mainly governed by the cross-section of the channel connecting the nozzle with outlet port (Figure 1). The microdevice used in this work had $10\ \mu\text{m}$ deep and $20\ \mu\text{m}$ wide channel, which confines liquid stream into pancake shape droplets. Due to fast mixing and

polymerization, the alginate stiffens rapidly into hydrogel particles that get locked in a biconcave shape (Figure 2 and Supplementary Figure S2). The size of such particles approaches the dimensions of mammalian cells ($\approx 5\ \mu\text{m}$ thick and $\approx 16\ \mu\text{m}$ wide) and therefore could find useful applications in biomedicine and pharmaceutical sectors. Although, the size of current particles precludes their wide use for drug delivery applications relying on a micrometer scale systems, yet the concept of “polymeric artificial cells” has been of interest not only as a means to deliver encapsulated compounds but also as a tool to modulate the in vivo response.^[25] Moreover, biocompatible particles, having $\approx 15\ \mu\text{m}$ size, could also find useful applications for in vivo delivery of the target cells ($\approx 6\text{--}8\ \mu\text{m}$ in size) or large bio-macromolecules (e.g., antibodies). In contrast, the use of larger ($\geq 30\ \mu\text{m}$) particles in vivo would be hardly possible due to clogging of the blood vessels. The use of cell-size particles as delivery systems could also benefit many other biomedical applications such as encapsulation of beneficial microorganisms,^[26] preparation of tumor vaccines,^[27] or triggering controlled immune response.^[28]

2.3. Encapsulation and Release

Alginate hydrogel particles suspended in water shows a delayed dissolution over the time window of 48 h (Figure 2, inset). This slow disintegration provides an attractive option to prolong the release of encapsulated biologicals and potentially enhance their therapeutic effect. We tested the release of FITC-labeled mouse IgG antibodies in more details. Droplets carrying encapsulated IgG were collected off-chip and after emulsification was complete, alginate particles were released from the emulsion by mixing it with 20% PFO (Figure 3a). The resulting particles were then

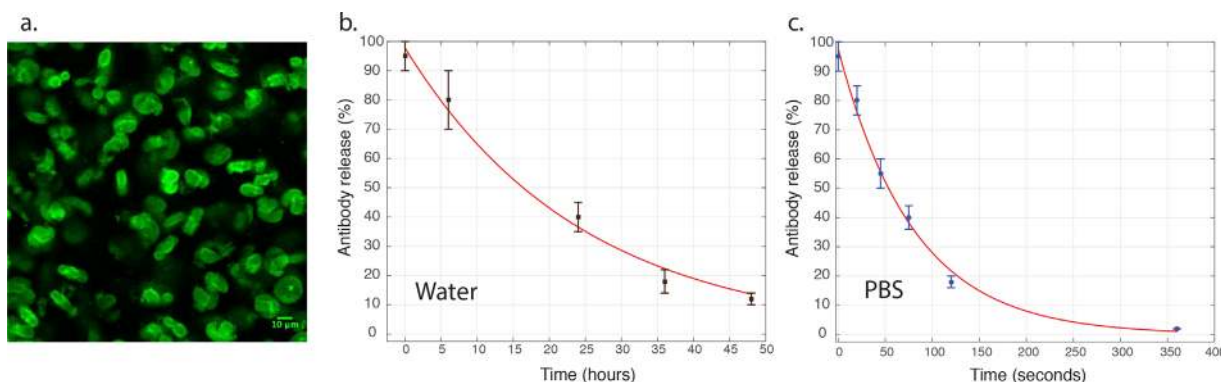


Figure 3. Antibody release from alginate-based hydrogel particles. Alginate particles ($n \approx 103$) carrying FITC labeled antibody were suspended in 1 mL water or 1 mL of PBS buffer and the fluorescence decay of individual particles monitored over time. (a) Fluorescence image of alginate particles immediately after mixing with water. (b) Antibody release from alginate particles suspended in water. (c) Antibody release from alginate particles suspended in 1x PBS buffer. The error bars denote standard deviation. Note the difference in time scale of antibody release. In phosphate buffered saline (PBS) buffer calcium forms ionic pair with phosphate that loosens hydrogel matrix.

dissolved in phosphate buffered saline ($1\times$ PBS) or pure water, and IgG release monitored over time with a fluorescence microscope. Based on existing literature data, our hydrogel particles have a pore size of $\approx 16\text{ nm}$ ^[29] and, therefore, the release of larger proteins (e.g., $\approx 20\text{ nm}$ in size) should be slowed in time. As expected, alginate particle dissolved in water slowly release encapsulated IgG over 36 h (Figure 3b). In contrast, antibody release in $1\times$ PBS was immediate (Figure 3c), presumably due to ion pair formation between Ca^{2+} and PO_4^{2-} groups resulting in a loose hydrogel matrix and thus fast IgG release. In mammalian serum, however, the free calcium concentration is $\approx 100\ \mu\text{g}/\text{mL}^{-1}$,^[30] an amount that would further reduce the alginate hydrogel dissolution. Finally, we tested the biocompatibility of alginate particles within biological fluids by mixing alginate particles ($n\approx 10^3$) carrying encapsulated antibodies with whole blood extracted from a mouse.

Alginate particles remained well dispersed in the whole blood with no signs of cell adherence to the surface of particles or of causing undesirable blood clogging (Figure 4). These results indicate that alginate particles are biocompatible and might be well suited for future biomedical applications. Subsequent research is necessary, however, for evaluation of release kinetics of antibodies from alginate particles into blood and slow particle dissolution, and our current efforts are dedicated to solve these tasks.

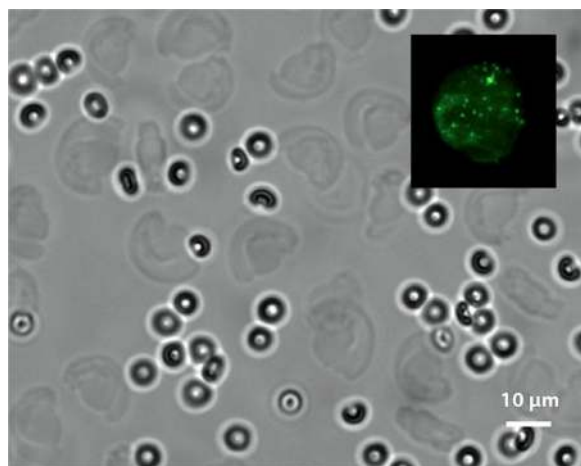


Figure 4. Alginate particle dissolution in mouse blood. Alginate particles containing encapsulated mouse antibody IgG were diluted in mouse blood and imaged under bright field microscope. Mouse erythrocytes (dark biconcave ellipses, $4\ \mu\text{m}$ in diameter) and alginate particles (light-grey biconcave ellipses, $\approx 15\ \mu\text{m}$ in diameter) remained well dispersed in a blood over the period of few hours without noticeable formation of agglomerates. Inset: single alginate particle containing encapsulated FITC-labeled antibody.

3. Conclusion

We have described a microfluidic approach that allows reliable production of alginate particles of unique, biconcave shape and sizes. By controlling the volume of alginate solution entering the droplet, we demonstrated the production of monodisperse biconcave particles approaching the dimensions of mammalian cells. Using triple flow microdevice, we have encapsulated antibodies and confirmed particle biocompatibility within blood samples. Due to slow degradation of alginate particles in aqueous fluids, the release of therapeutic compounds should be extended, therefore, providing a means to increase the biological action of therapeutics. We believe that the microfluidics approach provided in this work will be a useful addition to the existing tools for production of biopolymer-based drug carriers. Further reduction of alginate particle size down to $1\text{--}2\ \mu\text{m}$ size would be another useful step for development of natural and biodegradable drug delivery systems.

4. Experimental Section

4.1. Materials and Reagents

Sodium alginate from brown algae ($4\text{--}12\ \text{cP}$, 1% in H_2O), CaCl_2 and Phosphate buffered saline ($1\times$ PBS) were from Sigma–Aldrich and Roche. The water used in the experiments was deionized with a Millipore Purification system (Milli-Q). Carrier oil was FC-40 (3M) with 3% (w/w) fluorosurfactant. FITC-labeled mouse IgG was from Jackson ImmunoResearch. 1H,1H,2H,2H-Perfluorooctan-1-ol (PFO) was from Fluorochem Ltd.

4.2. Microfluidic Device Design and Fabrication

Rectangular microfluidic channels $10\ \mu\text{m}$ deep were fabricated using soft lithography. Briefly, the silicon wafer (University Wafers, Inc.) was coated with SU-8 2005 photoresist (Microchem Corp.) using a spin coater (Laurell) and exposed to UV light source (OAI) through the photolithography mask to create a master. The poly(dimethylsiloxane) (PDMS) mixture, containing PDMS base and the curing agent at $10:1$ ratio, was poured onto the master, degassed and cross-linked at $65\ ^\circ\text{C}$ for $\approx 12\ \text{h}$. The PDMS layer was then peeled off and access holes were punched with a $0.75\ \text{mm}$ diameter biopsy punch to create openings for inlet and outlet ports. The microchannels were sealed by bonding the PDMS slab to a glass slide after activation with an oxygen plasma (PlasmaPrep 2; GaLa Instrumente GmbH). The channels were treated with surface coating agent (Aquapel) to make them fluorophilic and subsequently flushed with nitrogen.

4.3. Microfluidic Device Operation

We used a microfluidic system where the flow regime was laminar with low Capillary and Reynold numbers, $\text{Ca}\approx 10^{-4}$ and $\text{Re}\approx 10^{-2}$,

respectively. The microfluidic device indicated in Figure 1 (see also Supplementary Information) consists of three inlets containing passive filters used to trap dust, followed by fluid resistors used to damp fluid fluctuations arising during operation of the device. The liquids from each inlet flow into a central channel of 80 μm long and 30 μm wide where they meet and flow in laminar flow, before being encapsulated into droplets. Emulsification of fluids occurs at flow-focusing junction, which has a short and narrow constriction of 10 μm wide and 10 μm long. The collection outlet is used to collect the droplets. The fluids were injected into the microfluidics chip via PTFE tubing ($0.56 \times 1.07 \text{ mm}^2$) connected to 1 mL syringes (Braun) and 25-gauge needles (Neolus). The flow rates of liquids and oil were controlled by syringe pumps (PHD 2000, Harvard Apparatus). The flow rate for aqueous phase was in the range of 20–50 $\mu\text{L} \cdot \text{h}^{-1}$ and for the continuous phase it was 100–300 $\mu\text{L} \cdot \text{h}^{-1}$. Emulsions were collected off-chip into a 1.5 mL tube. Droplet production was analyzed with a high-speed camera (Phantom V7.2) mounted on a Nikon Eclipse Ti-U microscope.

4.4. Alginate Particle Release from Microfluidic Droplets

Once droplet is generated the fast mixing between alginate and calcium ions induces immediate alginate gelation, which results in solid alginate particle occupying $\approx 80\%$ of droplet volume. To release alginate particles from the emulsion PFO was added on top of the emulsion to a final concentration of 10% (v/v) and incubated at room temperature for 5 min. The supernatant containing alginate particles was then transferred into a second tube for analysis.

4.5. Antibody Release Measurements

To study the antibody release, the solidified alginate particles (5 μL , $n \approx 10^5$) carrying FITC-labeled IgG were suspended in 1 500 μL phosphate buffered saline buffer ($1 \times \text{PBS}$, pH [7.4]) or MQ-water. The room temperature was controlled by air conditioner at $22 \pm 1^\circ\text{C}$. At selected time points, 10 μL sample ($\approx 10^2$ particles) was sandwiched between the microscope slide and cover slip and green fluorescence of the alginate particles was recorded using Leica confocal microscope (TCS SP5) and 488 nm laser. The emission light at $532 \pm 20 \text{ nm}$ was recorded with PMT embedded inside the microscope system. For each data point ≈ 20 –30 randomly chosen alginate particles were analyzed using Microscope imaging software by Leica Microsystems to extract the mean fluorescence intensity and standard deviation values. The mean fluorescence intensity of the particles at incubation time 0 was set as 100% (y -axis in Figure 3), followed by subsequent measurements at selected time points.

Acknowledgements: We are grateful to Dovile Dekaminaviciute for supplying us with a sample of mouse blood. This work was supported by Lithuanian Agency for Science, Innovation and Technology (MITA, uVesicles 31v-40). R.V. holds postdoctoral fellowship from the European Union Structural Funds project "Postdoctoral Fellowship Implementation in Lithuania" (VP1-3.1-SMM-01).

Received: June 10, 2015; Revised: June 22, 2015; Published online: DOI: 10.1002/mabi.201500226

Keywords: alginate particles; droplet microfluidics; antibody; drug delivery system

- [1] J. W. Yoo, D. J. Irvine, D. E. Discher, S. Mitragotri, *Nat. Rev. Drug Discov.* **2011**, *10*, 521.
- [2] K. A. Smith, J. M. Ottino, M. O. de la Cruz, *Phys. Rev. Lett.* **2004**, *93*, 204501.
- [3] J. Tu, S. Bolla, J. Barr, J. Miedema, X. Li, B. Jasti, *Int. J. Pharm.* **2005**, *303*, 171.
- [4] W. J. Duncanson, T. Lin, A. R. Abate, S. Seiffert, R. K. Shah, D. A. Weitz, *Lab Chip* **2012**, *12*, 2135.
- [5] G. F. Christopher, S. L. Anna, *J. Phys. D Appl. Phys.* **2007**, *40*, R319.
- [6] A. R. Abate, J. Thiele, D. A. Weitz, *Lab Chip* **2011**, *11*, 253.
- [7] L. Y. Chu, J. W. Kim, R. K. Shah, D. A. Weitz, *Adv. Funct. Mater.* **2007**, *17*, 3499.
- [8] Q. Xu, M. Hashimoto, T. T. Dang, T. Hoare, D. S. Kohane, G. M. Whitesides, R. Langer, D. G. Anderson, *Small* **2009**, *5*, 1575.
- [9] C. Alvarez-Lorenzo, B. Blanco-Fernandez, A. M. Puga, A. Concheiro, *Adv. Drug Deliv. Rev.* **2013**, *65*, 1148.
- [10] P. Eisele, J. Yeh, R. K. Latvala, L. D. Shea, D. J. Mooney, *Biomaterials* **2000**, *21*, 1921.
- [11] K. Y. Lee, M. C. Peters, K. W. Anderson, D. J. Mooney, *Nature* **2000**, *408*, 998.
- [12] K.-S. Huang, Y.-S. Lin, C.-H. Yang, C.-W. Tsai, M.-Y. Hsu, *Soft Matter* **2011**, *7*, 6713.
- [13] L. Capretto, S. Mazzitelli, C. Balestra, A. Tosi, C. Nastruzzi, *Lab Chip* **2008**, *8*, 617.
- [14] W. Y. Chen, J. H. Kim, D. Zhang, K. H. Lee, G. A. Cangelosi, S. D. Soelberg, C. E. Furlong, J. H. Chung, A. Q. Shen, *J. R. Soc. Interface* **2013**, *10*, 20130566.
- [15] L. Liu, F. Wu, X.-J. Ju, R. Xie, W. Wang, C. H. Niu, L.-Y. Chu, *J. Colloid Interface Sci.* **2013**, *404*, 85.
- [16] L. B. Zhao, L. Pan, K. Zhang, S. S. Guo, W. Liu, Y. Wang, Y. Chen, X. Z. Zhao, H. L. W. Chan, *Lab Chip* **2009**, *9*, 2981.
- [17] W.-H. Tan, S. Takeuchi, *Adv. Mater.* **2007**, *19*, 2696.
- [18] V. L. Workman, S. B. Dunnett, P. Kille, D. D. Palmer, *Macromol. Rapid Commun.* **2008**, *29*, 165.
- [19] M. Lian, C. P. Collier, M. J. Doktycz, S. T. Retterer, *Biomicrofluidics* **2012**, *6*, 044108.
- [20] J. H. Xu, S. W. Li, J. Tan, G. S. Luo, *Chem. Eng. Technol.* **2008**, *31*, 1223.
- [21] T. Braschler, A. Valero, L. Colella, K. Pataky, J. Brugger, P. Renaud, *Anal. Chem.* **2011**, *83*, 2234.
- [22] D. Saeki, S. Sugiura, T. Kanamori, S. Sato, S. Ichikawa, *Lab Chip* **2010**, *10*, 2292.
- [23] L. Mazutis, J. C. Baret, A. D. Griffiths, *Lab Chip* **2009**, *9*, 2665.
- [24] H. Zhang, E. Tumarkin, R. Peerani, Z. Nie, R. M. a. Sullan, G. C. Walker, E. Kumacheva, *J. Am. Chem. Soc.* **2006**, *128*, 12205.
- [25] T. M. S. Chang, *Nat. Rev. Drug Discov.* **2005**, *4*, 221.
- [26] B. J. Kim, T. Park, H. C. Moon, S. Y. Park, D. Hong, E. H. Ko, J. Y. Kim, J. W. Hong, S. W. Han, Y. G. Kim, I. S. Choi, *Angew. Chem. Int. Ed. Engl.* **2014**, *53*, 14443.
- [27] W. A. Li, D. J. Mooney, *Curr. Opin. Immunol.* **2013**, *25*, 238.
- [28] J. Kim, W. A. Li, Y. Choi, S. A. Lewin, C. S. Verbeke, G. Dranoff, D. J. Mooney, *Nat. Biotechnol.* **2015**, *33*, 64.
- [29] K. I. Draget, G. S. Braek, O. Smidsrod, *Carbohydr. Polym.* **1994**, *25*, 31.
- [30] J. F. Sullivan, A. J. Blotcky, M. M. Jetton, H. K. J. Hahn, R. E. Burch, *J. Nutr.* **1979**, *109*, 1432.